Investigation of the Substituent Effects on π-Type Pnicogen Bond Interaction

XU Hui-Ying(许惠英)[1];CAO Sheng-Wei(曹生炜)[2];WANG Wei(王 维)[3];ZHU Jian-Qing(朱建清)[4];ZOU Jian-Wei(邹建卫)[5];XU Xiao-Lu(许晓路)[1]LU Yin(陆胤)[1]

[1] (*College of Biology & Environment Engineering, Zhejiang Shuren University, Hangzhou* 310015, *China*;[2]*Zhejiang Linix Motor CO., LTD, Dongyang* 322118, *China*;[3]*Zhejiang Surveying Institute of Estuary and Coast, Hangzhou* 310008, *China*;[4]*Department of Basic Courses, Zhejiang Shuren University, Hangzhou* 310015, *China*;[5]*Ningbo Institute of Technology, Zhejiang University, Ningbo* 315104, *China*

ABSTRACT Intermolecular interactions between PH_2Cl and Ar–R (R = H, OH, NH_2, CH_3, Br, Cl, F, CN, NO_2) were calculated by using MP2/aug-cc-pVDZ quantum chemical method. It has been shown from our calculations that the aromatic rings with electron-withdrawing groups represent much weaker binding affinities than those with electron-donating groups. The charge-transfer interaction between PH_2Cl and Ar–R plays an important role in the formation of pnicogen bond complexes, as revealed by NBO analysis. Nevertheless, AIM analysis shows that the nature of the interactions between PH_2Cl and Ar–R is electrostatic, and the interaction energies of the complexes are correlated positively with the electron densities in the bond critical points (BCPs). RDG/ELF graphical analyses were performed to visualize the positions and strengths of the pnicogen bonding, as well as the spatial change of the electron localization upon the formation of complexes. The π-type halogen bond was also calculated, and it has been revealed that the π-type pnicogen bond systems are more stable than the halogen bond ones.

Keywords: π-type pnicogen bonding; π-type halogen bonding; NBO; AIM; RDG/ELF analysis; DOI: 10.14102/j.cnki.0254-5861.2011-1745

1 INTRODUCTION

Molecular interaction, closely correlated to various physicochemical properties, life phenomena and material structures, has been of great concern in physics, chemistry, biology, material science and some other fields[1-5]. The hydrogen bond interaction is of typical molecular interaction[6]. Then, the halogen bond[7], lithium bond[8] and other weak interaction were found. In

2009, Hey-Hawkins et al[9] proved the existence of P···P non-bond interaction via ^{13}C {^{1}H, ^{31}P} NMR experiment. Scheiner[10-15] theoretically calculated the geometrical structure and interaction energy of a series of pnicogen bond systems including P···P, N···P, etc. Since then, the research on pnicogen bond interaction has attracted the attention of theoretical and experimental chemists[16-20]. Recently, Zukerman-Schepector et al[21] emphatically discussed the As···π interaction of the supermolecular system, searched out 20 structures involved with the As···π interaction from the CSD (Cambridge Structural Database), and concluded the importance of As···π interaction in supermolecular construction from these characteristic structures. Based on the achievement of Zukerman-Schpector, et al, the interaction was calculated between ECl_3 (E = As, Sb, Bi) and π electron donors (e.g. benzene, hexafluorobenzene) by Frontera subject team[22], and the significance of π-type pnicogen bond in the life science field was explored. PH_3 is the simplest pnicogen-bond donor molecule with a weak pnicogen bond interaction. However, when one of the H atoms is replaced by Cl atom (PH_2Cl), the P···N pnicogen bonding interaction formed between PH_2Cl and the representative electron donor NH_3 even exceeds the hydrogen bond interaction between water molecules[23], so PH_2Cl is often used as the model molecule in the research on pnicogen bond interaction[24, 25]. In this paper, the interactions between PH_2Cl and the substituted benzene (Ar–R, R = H, OH, NH_2, CH_3, Br, Cl, F, CN, NO_2) are calculated using the quantum chemistry method, aiming to explore the geometrical structure, electronic structure and interaction energy of π-type pnicogen bond between PH_2Cl and the aromatic compound. Furthermore, the effects of the substituting group in the aromatic ring to the stability of π-type pnicogen bond complex are considered, in order to provide a theoretical basis for recognizing the nature of π-type pnicogen bonds.

2 COMPUTATIONAL METHODS

The structure optimizations and energy calculations of all molecules are performed by Gaussian 03[26] program package. Considering the importance of electron correlation for accurate expression of interaction energy, the structure optimizations of all monomers and complexes are performed by MP2 method with aug-cc-pVDZ basis set, and no symmetry limit is applied to the optimization. It has also been proved that this method is applicable in the research on pnicogen bond interaction[27, 28]. The interaction energy (ΔE_{int}), obtained from the complex energy deducting two monomer energies, is corrected to interaction energy (ΔE_{int}^{CP}) through the BSSE (Basis set superposition error) correction by CP (counterpoise) procedure[29]. To further investigate the geometric and electronic properties of the complex systems, the second-order perturbation stabilization energy (ΔE^2) and the charge transfer quantity are calculated by the NBO program in the Gaussian 03 program package. Meanwhile, the topological properties at BCP (Bond Critical Point) are calculated by the program AIM 2000, and the RDG/ELF (Reduced Density Gradient and Electron

Localization Function) is obtained by the Multiwfn software developed by Lu, et al[30], and used to analyze these systems.

3 RESULTS AND DISCUSSION

3. 1 Geometrical structure and interaction energy

The stable structures of the complexes combining PH_2Cl with substituted aromatic compounds are obtained at the level MP2/aug-cc-pVDZ, and the geometrical structures are shown as Fig. 1. As can be seen from these geometrical structures in Fig. 1, the pnicogen bond interaction is generated between the P atom in PH_2Cl and the π-electron in the aromatic ring. According to our aforesaid definitions[31], the α angle is the included angle between the vector from the P atom to the hetero ring centroid and the vector at the P–Cl bond direction (see Fig. 2), and the values of angle α for complexes **1**～**9** are shown in Table 1. The angle α values of 8 complexes are almost 180 °except that of complex **3**, i.e. the three points of Cl, P, and the centroid are almost at the same straight line. The optimization result for complex **3** shows that one of the H atoms (H17) in PH_2Cl is also close to the aromatic ring center, i.e. a certain π-type hydrogen bond interaction is formed between the atom H in PH_2Cl and the π-electron in the aromatic ring, so the decrease of angle α is caused by the interference of interaction P(15)–H(17) $\cdots\pi$.

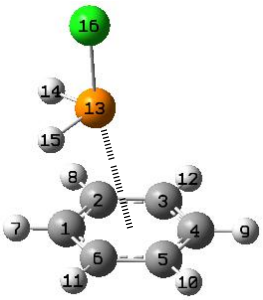

Complex **1**

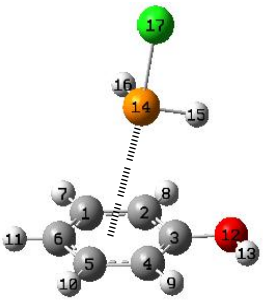

Complex **2**

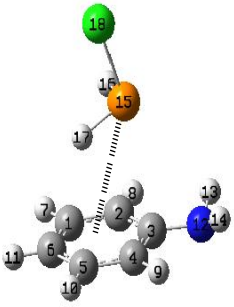

Complex **3**

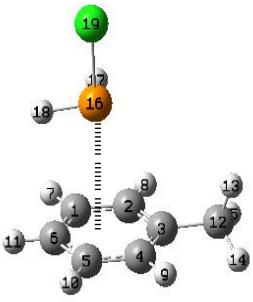

Complex 4

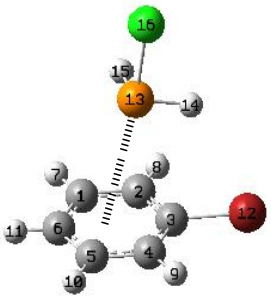

Complex 5

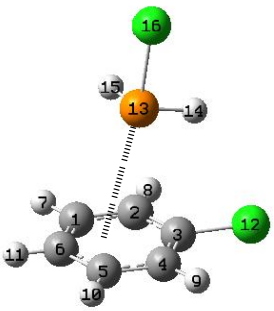

Complex 6

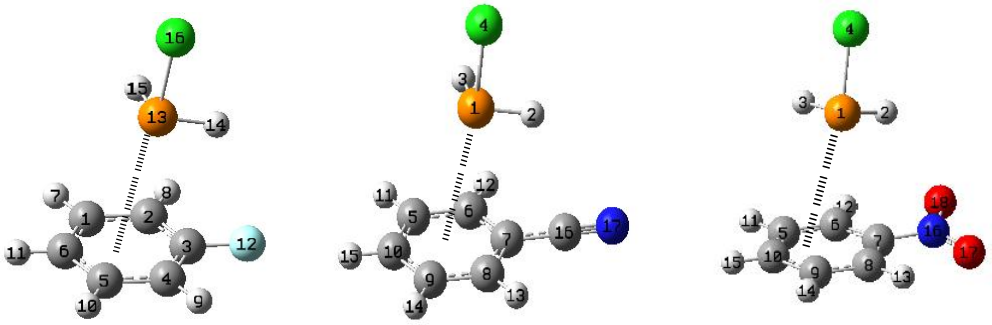

Complex 7 Complex 8 Complex 9

Fig. 1. Optimized geometries of complexes at the MP2/ aug-cc-pVDZ level

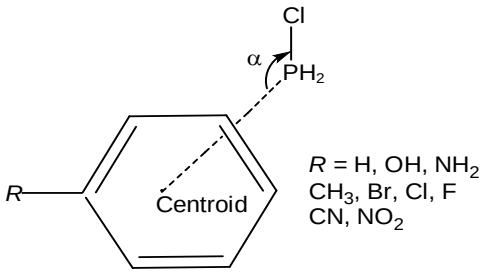

Fig. 2. Geometric model of the pnicogen bonded angle *α*

The uncorrected interaction energies (ΔE_{int}) and the corrected interaction energies (ΔE_{int}^{CP}) of the complexes obtained at the MP2/ aug-cc-pVDZ level are listed in Table 1. Comparing the $\Delta \boldsymbol{E}_{int}$ with ΔE_{int}^{CP}, the differences between them are 2.7 to 3.5 kcal·mol^{-1}, so BSSE correction is necessary for the π-type pnicogen bond systems. Complex **1** is the one formed by PH_2Cl and the non-substituted benzene, whose corrected interaction energy is –3.81 kcal·mol^{-1}. The corrected interaction energies of complexes **2** and **3** are –7.56 and –9.65 kcal·mol^{-1}, respectively, which are much larger than that of complex **1**. As the substituted groups -OH and -NH_2 are electron donor ones, the electron density of π-electron system in the benzene ring is increased, which then leads to a stronger interaction between PH_2Cl and π-electron, greater interaction energy of the complex and a more stable complex. Similarly, the electron donating capacity of the group -CH_3 is weaker than the above two, so the interaction energy of complex **4** is smaller than that of **2** and **3**. The corrected interaction energies of complexes **7**～**9** are –3.55, –3.44, and –3.45 kcal·mol^{-1}, respectively, which are smaller than the interaction energy of complex **1**, i.e. complexes **7**～**9** are less stable than **1**. This is because the electron-withdrawing groups, -F, -CN and -NO_2, reduce the π-electron density in the benzene ring, and result in the weakening of the interaction between P and π-electron. It is worth noting that the substituting groups -Br and -Cl in complexes **5** and **6** are electron-withdrawing groups, but their interaction energies are a little larger than that of complex **1**. The reason may be the weak hydrogen bond interaction between the hydrogen atom in PH_2Cl and halogen atom of the substituting group. It can be clearly seen in the geometrical structure of

Fig. 1, and also proven by the following NBO analysis.

The halogen bond is the interaction between the electron donor and the halogen atom in the halogenous molecule. It was found earlier than the pnicogen bond, and the research on halogen bonds is more mature than the pnicogen bond. In our current research system, when the π-type pnicogen bond interaction can be generated between the PH_2Cl molecule and the aromatic compound, a π-type halogen bond complex can be generated between π electron of the aromatic ring and atom Cl in the PH_2Cl molecule. As a comparison, the molecular structures of nine typical halogen bond complexes are optimized at the MP2/aug-cc-pVDZ level, and then their corrected interaction energies (ΔE_{XB}^{CP}), corrected through the BSSE, are shown in Table 1. Comparing the corrected interaction energy $\Delta E_{\text{int}}^{CP}$ of the pnicogen bond system and the corrected interaction energy (ΔE_{XB}^{CP}) of the corresponding halogen bond system, it has been found that the π-type pnicogen bond system is more stable than the π-type halogen bond system. It is caused by the unbalanced distribution of positive electrostatic potential in the PH_2Cl. The structures of two representative halogen bond complexes are shown in Fig. 3, where the positive electrostatic potential at the top of atom P is larger than that at the top of atom Cl in the same aromatic π electron donor.

Table 1. Geometric Parameters and Interaction Energies of the Complexes at the MP2/aug-cc-pVDZ level[a]

Pnicogen bonding complexes	ΔE_{int}	$\Delta E_{\text{int}}^{CP}$	α (°)	Halogen bonding complexes	ΔE_{XB}^{CP}
Complex **1** ($H_2ClP\cdots Ar–H$)	–6.54	–3.81	169.1	$PH_2Cl\cdots Ar–H$	–1.58
Complex **2** ($H_2ClP\cdots Ar–OH$)	–10.66	–7.56	169.3	$PH_2Cl\cdots Ar–OH$	–4.99
Complex **3** ($H_2ClP\cdots Ar–NH_2$)	–13.09	–9.65	145.6	$PH_2Cl\cdots Ar–NH_2$	–6.00
Complex **4** ($H_2ClP\cdots Ar–CH_3$)	–7.19	–4.28	167.1	$PH_2Cl\cdots Ar–CH_3$	–2.09
Complex **5** ($H_2ClP\cdots Ar–Br$)	–7.57	–4.12	171.5	$PH_2Cl\cdots Ar–Br$	–2.05
Complex **6** ($H_2ClP\cdots Ar–Cl$)	–7.22	–4.05	170.1	$PH_2Cl\cdots Ar–Cl$	–1.97
Complex **7** ($H_2ClP\cdots Ar–F$)	–6.49	–3.55	171.8	$PH_2Cl\cdots Ar–F$	–1.82
Complex **8** ($H_2ClP\cdots Ar–CN$)	–6.43	–3.44	168.8	$PH_2Cl\cdots Ar–CN$	–2.35
Complex **9** ($H_2ClP\cdots Ar–NO_2$)	–6.63	–3.45	170.1	$PH_2Cl\cdots Ar–NO_2$	–2.74

[a] Interaction energies are given in kcal·mol^{-1}.

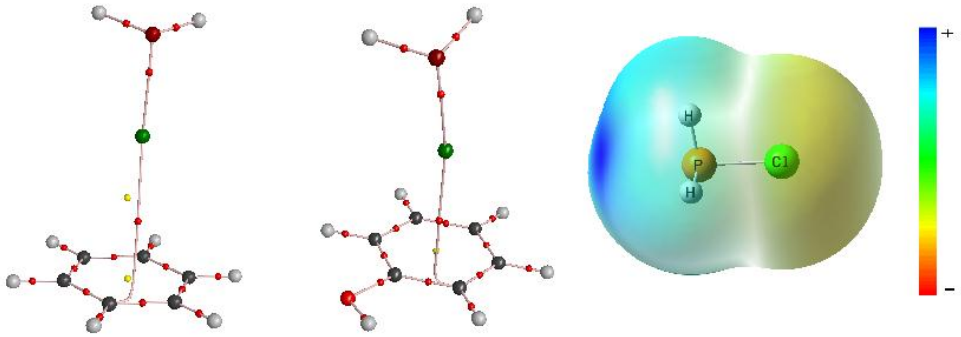

$PH_2Cl\cdots Ar–H$ **$PH_2Cl\cdots Ar–OH$** **Monomers PH_2Cl**

Fig. 3. Molecular graphs of $PH_2Cl\cdots Ar–H$ and $PH_2Cl\cdots Ar–OH$ and electrostatic potential surface of monomers PH_2Cl

3. 2 NBO analysis

Table 2 shows the donor-acceptor orbital, the second-order perturbation stabilization energy (ΔE^2), and the charge transfer quantum (Q_{CT}) of 9 π-type pnicogen bond complexes at the level MP2/aug-cc-pVTZ. The second-order perturbation stabilization energy (ΔE^2) can be obtained from the following equation:

$$\Delta E^2 = \Delta E_{ij} = q_i \frac{F(i,j)^2}{\varepsilon_j - \varepsilon_i}$$

where q_i is the donor orbital occupancy, ε_i and ε_j are the diagonal elements (orbital energies), and F is the NBO Fock matrix element. It has been shown from the donor-acceptor orbital for complexes **1**～**9** in Table 2 that the pnicogen bonding interaction is mainly the interaction between the C–C π bonding orbital and the σ anti-bonding orbital of P–Cl in the monomer PH_2Cl. The three complexes **3**, **5** and **6** are further involved with the hydrogen bond interaction in addition to the pnicogen bond interaction. The second-order perturbation stabilization energy values indicate that the pnicogen bond interaction, followed by the hydrogen bond interaction, plays a key role in the complex stability. The existence of the supportive hydrogen bond interaction is the fact that complexes **5** and **6** have higher interaction energies than complex **1** in the above analysis, and why the angle α is smaller in complex **3**.

Table 2. Natural Bond Orbital Analysis of Complexes 1～9 at the MP2/aug-cc-pVDZ Level

Complexes	Donor NBOs	Acceptor NBOs	ΔE^2/kcal.mol^{-1}	Q_{CT}/e
Complex **1** ($H_2ClP\cdots Ar–H$)	BD (2) C(1)–C(6) BD (2) C(2)–C(3)	BD* (1) P(13)–Cl(16)	3.05 0.56	0.01115
Complex **2** ($H_2ClP\cdots Ar–OH$)	BD (2) C(1)–C(6) BD (2) C(2)–C(4)	BD* (1) P(14)–Cl(17)	3.50 0.62	0.01536
Complex **3** ($H_2ClP\cdots Ar–NH_2$)	BD (2) C(2)–C(3) BD (2) C(1)–C(6)	BD* (1) P(15)–Cl(18) BD* (1) H(17)–P(15)	4.47 1.02	0.01614

Complex **4** ($H_2ClP\cdots Ar–CH_3$)	BD (2) C(1)–C(6) BD (2) C(2)–C(3)	BD* (1) P(16)–Cl(19)	2.30 1.10	0.01007
Complex **5** ($H_2ClP\cdots Ar–Br$)	BD (2) C(2)–C(3) Lp (3)Br(12)	BD* (1) P(13)–Cl(16) BD* (1) H(14)–P(13)	2.85 0.81	0.01250
Complex **6** ($H_2ClP\cdots Ar–Cl$)	BD (2) C(2)–C(3) Lp (3)Cl(12)	BD* (1) P(13)–Cl(16) BD* (1) H(14)–P(13)	2.91 0.49	0.01179
Complex **7** ($H_2ClP\cdots Ar–F$)	BD (2) C(2)–C(6) BD (2) C(1)–C(6)	BD* (1) P(13)–Cl(16)	3.06 0.43	0.01077
Complex **8** ($H_2ClP\cdots Ar–CN$)	BD (2) C(6)–C(7)	BD* (1) P(1)–Cl(4)	2.78	0.00643
Complex **9** ($H_2ClP\ldots Ar–NO_2$)	BD (2) C(5)–C(6) BD (2) C(7)–C(8)	BD* (1) P(1)–Cl(4)	2.30 0.57	0.00953

According to the data in Table 2, the correlation between the second-order perturbation stabilization energy of the C–C π bonding orbital and the σ anti-bonding orbital of P–Cl and the corrected interaction energy are mapped in Fig. 4(a), and the following relational expression is obtained after fitting:

$$\Delta E_{\text{int}}^{CP} = -37.0697 + 21.5691\Delta E^2 - 3.46391(\Delta E^2)^2$$

$$R = 0.956,\ \text{SD} = 0.527,\ N = 9$$

The curve in Fig. 4(a) shows there is a bi-variable function relation between the second-order perturbation stabilization energy (ΔE^2) of the C–C π bonding orbital and the σ anti-bonding orbital of P–Cl and the corrected interaction energy ($\Delta E_{\text{int}}^{CP}$), other than the traditional linear relation, and it also shows the contribution of pnicogen bond interaction to the complex stability. In consideration of the factors of hydrogen bond interaction in the other three complexes, the second-order perturbation stabilization energy of hydrogen bond interaction is combined with the one of π-type pnicogen bond interaction, and the relationship between the combined second-order perturbation stabilization energy (ΔE^2) and their corrected interaction energy ($\Delta E_{\text{int}}^{CP}$) is further mapped in Fig. 4(b). The correlation chart in Fig. 4(b) shows that the combined ΔE^2 is linear to their interaction energy with the correlation coefficient (R) of 0.924, i.e. the weak interactive second-order perturbation stabilization energy (ΔE^2) is positively correlated to the complex stability.

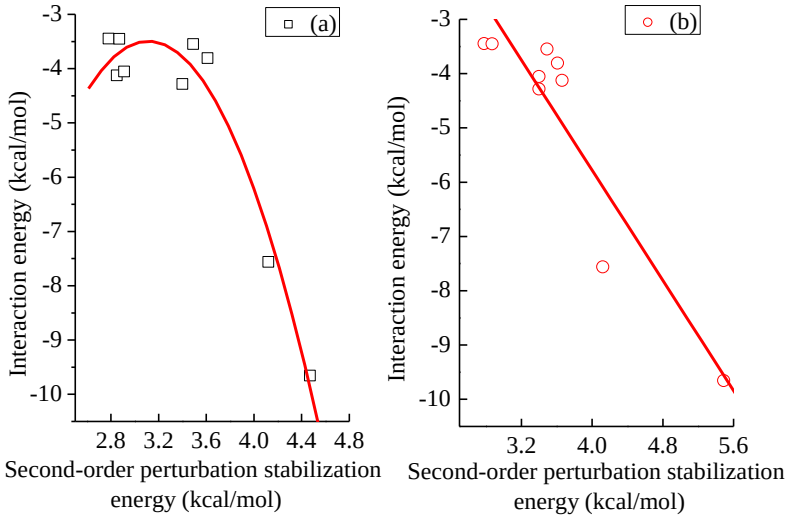

Fig. 4. Relationship between the second-order perturbation stabilization energy and interaction energy

The molecular interaction is always accompanied by charge transfer, whose quantities in complexes **1**～**9** are shown in Table 2. As seen in the table, the charge quantities transferred from the aromatic compound to PH_2Cl molecule are from 6 to 16me. The charge quantity transferred is not so much, and it complies with the soft acid-soft alkali model (PH_2Cl molecule as the soft acid and the aromatic compound as the soft alkali). The plot of the charge transfer quantity and the corrected interaction energy is shown in Fig. 5. The curvilinear equation is as below:

$$\Delta E_{\text{int}}^{CP} = -11.215 + 1852.819\, Q_{\text{CT}} - 106824.298\, (Q_{\text{CT}})^2$$

$$R = 0.954,\ \text{SD} = 0.540,\ N = 9$$

Fig. 5 shows that the charge transfer quantities of the 9 complexes decrease with their interaction energies decreasing, and this result indicates that the charge transfer plays an important role in the complex stability.

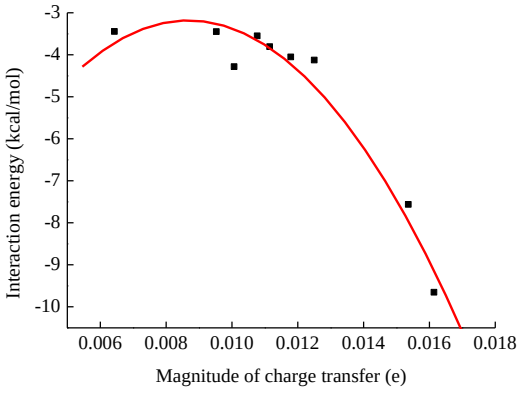

Fig. 5. Relationship between charge transfer and interaction energy

3. 3 AIM analysis

To further analyze the nature of π-type pnicogen bond interaction, the AIM (Atom in Molecule) theory developed by Bader is used, as the theory is often used in researches on molecular weak interactions[32-35]. The typical pnicogen bond complex molecular diagram has been shown in Fig. 6, in which a critical point between the atom P and the aromatic ring is observed, and therefore the existence of π-type pnicogen bonds is proved. Table 3 shows the electron densities (ρ_b), Laplacian of electron densities ($\nabla^2\rho_b$), three eigenvalues (λ_1, λ_2, λ_3) of Hessian matrix, kinetic energy densities (G_b), potential energy densities (V_b) and electronic energy density (H_b) of the 9 π-type pnicogen bond complexes at the bond critical point of pnicogen bond (BCP) at the MP2/aug-cc-pVDZ level.

According to the AIM theory, charges are dispersed and the bond ionicity is stronger at BCP when $|\lambda_1 + \lambda_2| < \lambda_3$ and $\nabla^2\rho_b > 0$, but charges are centralized and the bond covalence is stronger when $|\lambda_1 + \lambda_2| > \lambda_3$ and $\nabla^2\rho_b < 0$. The data in Table 3 suggest that, the Laplacian quanta ($\nabla^2\rho_b$) at BCP are larger than zero and $|\lambda_1 + \lambda_2| < \lambda_3$, which means the ionicity of π-type pnicogen bond is stronger in complexes **1**～**9**. The electronic energy density H_b (sum of the kinetic energy density G_b and the potential energy density V_b) is often deemed as a correct index for understanding the weak interaction[36, 37]. The interaction is a static interaction when $H_b > 0$, and is a covalence interaction when $H_b < 0$. All H_b values in Table 3 are larger than zero, which means that the interactions of the 9 π-type pnicogen bond complexes belong to the static interaction, and it complies with the above conclusion that "charges are dispersed and the bond ionicity is stronger at BCP when $|\lambda_1 + \lambda_2| < \lambda_3$ and $\nabla^2\rho_b > 0$". The electron density (ρ_b) at BCP is correlated to the bond strength, as the bond strength is larger if the electron density is higher. The relationship of the electron density (ρ_b) at BCP and the corrected interaction energy of the complex is mapped (Fig. 7), and the correlation coefficient R is 0.915.

Table 3. Topological Parameters of Complexes 1～9 at the BCP Point[b]

Complexes	ρ_b	$\nabla^2\rho_b$	λ_1	λ_2	λ_3	G_b	V_b	H_b
Complex **1** ($H_2ClP\cdots Ar–H$)	0.0103	0.0277	–0.0055	–0.0014	0.0346	0.0062	–0.0054	0.0008
Complex **2** ($H_2ClP\cdots Ar–OH$)	0.0121	0.0321	–0.0061	–0.0025	0.0408	0.0072	–0.0064	0.0008
Complex **3** ($H_2ClP\cdots Ar–NH_2$)	0.0122	0.0307	–0.0064	–0.0035	0.0406	0.0069	–0.0061	0.0008
Complex **4** ($H_2ClP\cdots Ar–CH_3$)	0.0105	0.0272	–0.0055	–0.0017	0.0344	0.0060	–0.0051	0.0008
Complex **5** ($H_2ClP\cdots Ar–Br$)	0.0108	0.0303	–0.0054	–0.0011	0.0368	0.0067	–0.0058	0.0009
Complex **6** ($H_2ClP\cdots Ar–Cl$)	0.0110	0.0305	–0.0055	–0.0014	0.0374	0.0067	–0.0058	0.0009

Complex **7** ($H_2ClP\cdots Ar–F$)	0.0107	0.0293	–0.0055	–0.0013	0.0361	0.0065	–0.0057	0.0008
Complex **8** ($H_2ClP\cdots Ar–CN$)	0.0101	0.0279	–0.0051	–0.0012	0.0342	0.0061	–0.0052	0.0009
Complex **9** ($H_2ClP\cdots Ar–NO_2$)	0.0108	0.0298	–0.0054	–0.0017	0.0369	0.0065	–0.0055	0.0010

[b] Topological parameters are given in a.u.

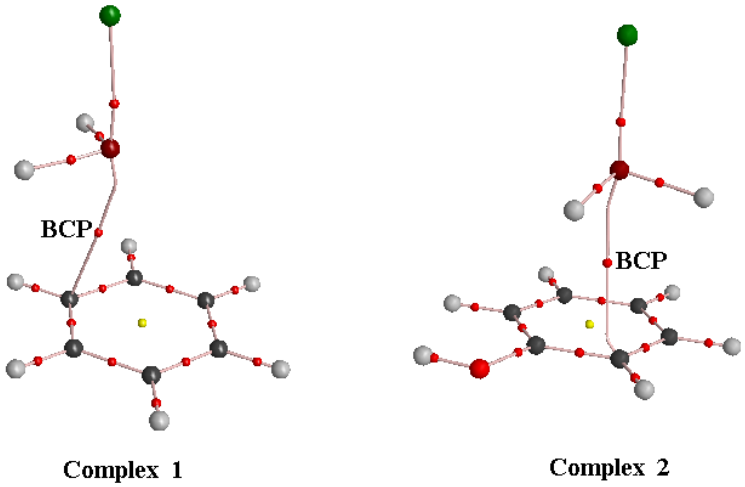

Fig. 6. Molecular graphs of complexes 1 and 2

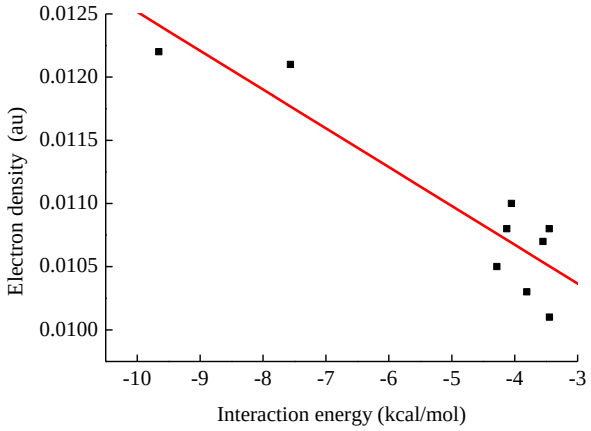

Fig. 7. Relationship between the electron density at BCPs and interaction energy

3. 4 RDG/ELF analysis

Yang Weitao's subject team[38] has developed a visualized method for the weak interaction research, through which the calculated values of reduced density gradient (RDG) function and sign $(\lambda_2(r))\rho(r)$ of each point in the space are visualized in the RDG isosurface map. The gradient isosurfaces are colored according to the corresponding values of sign $(\lambda_2(r))\rho(r)$, which is found to be a good indicator of interaction strength. We used this method in analyzing the position and strength of the interaction between hydrogen bonds, halogen bonds and pnicogen bonds and the coordination bond, and the result was promising[39-41]. The electron localization function (ELF) is

an important tool for electron structure researches, and it is often used to study chemical problems[42] such as the molecular interaction. These two analysis methods are applied to π-type pnicogen bond interaction in order to visualize the interaction change.

Fig. 8 shows the isosurface map for complexes **1** and **2** obtained from the combination of RDG and ELF (Fig. 8a) and the electron localization isosurface map of PH_2Cl (Fig. 8b). In the case, the spatial position of molecular interaction can be expected, and the interaction strength is also observed according to the color of RDG map, in which blue represents the strong interaction, green the weak interaction, and red the repulsion. Comparing the color-filled RDG isosurface maps for complex **1** and complex **2**, we can find the blue zone of complex **2** is deeper than that of complex **1**, which suggests complex **2** has stronger pnicogen bond interaction than **1**. The white column and vacuum ring zones in Fig. 8a represent the localization spaces of the lone-pair electron, π electron and valence electron. The localization space (V(P)) of the lone-pair electron on the atom P is obviously weakened (Fig. 8b). The reason for such phenomenon is that the intermolecular distance is shortened by the weak interaction, and some repulsion is generated between π electron and the lone-pair electron on the atom P. Such weak interaction force shortening the intermolecular distance is mainly the static interaction. According to the AIM analysis, the pnicogen bond interaction is mainly the static acting force. In other words, what is weakening the lone-pair electron localization space on P atom is the pnicogen bond interaction to a certain extent.

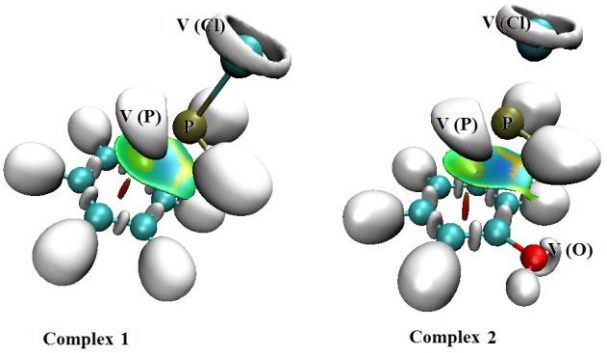

(a)

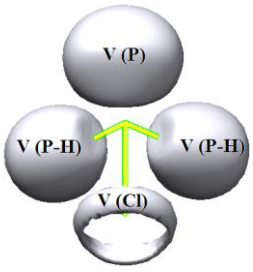

(b)

Fig. 8. (a) RDG/ELF isosurface map of complexes 1 and 2; (b) ELF isosurface map (η = 0.9) of PH_2Cl

4 CONCLUSION

The geometrical structural optimization, energy calculation and topological and graphic analyses for the various pnicogen bond system of PH_2Cl and Ar–R (R = H, OH, NH_2, CH_3, Br, Cl, F, CN, NO_2) have been made at level MP2/aug-cc-pVDZ. The results showed that the complex pnicogen bond interaction is strengthened when the substituting group in the benzene ring is the electron donating group, and the complex pnicogen bond interaction is weakened when the substituting group is the electron withdrawing group. To compare the interaction energy of the π-type pnicogen bond system with the halogen bond system, the interaction energy of π-type halogen bond system is also calculated, and it is showed that the π-type pnicogen bond system is more stable. NBO theory is used to analyze the correlation between the second-order perturbation stabilization energy and the charge transfer quantum with the interaction energy, and the result shows that the charge transfer plays an important role in the stability of the pnicogen bond complex. AIM analysis has indicated that, the nature of pnicogen bond interaction is the electrostatic interaction, and the electron density at BCP is positively correlated to the interaction energy of the pnicogen bond complex. RDG analysis showed the position and strength of pnicogen bond interaction, and ELF analysis indicated the change of lone-pair electron localization space on P atom after the complex formation.

REFERENCES

(1) Nguyen, H. L.; Horton, P. N.; Hursthouse, M. B.; Legon, A. C.; Bruce, D. W. Halogen bonding: a new interaction for liquid crystal formation. *J. Am. Chem. Soc.* **2004**, 126, 16-17.

(2) Baiocco, P.; Colotti, G.; Franceschini, S.; Ilari, A. Molecular basis of antimony treatment in Leishmaniasis. *J. Med. Chem*. **2009**, 52, 2603-2612.

(3) Gillet, N.; Chaudret, R.; Contreras-Garc á, J.; Yang, W.; Silvi, B.; Piquemal, J. Coupling quantum interpretative techniques: another look at chemical mechanisms in organic reactions. *J. Chem. Theory Comput*. **2012**, 8, 3993-3997.

(4) Mahadevi, A. S.; Sastry, G. N. Cation-π interaction: its role and relevance in chemistry, biology, and material science. *Chem. Rev*. **2013**, 113, 2100-2129.

(5) Schneider, H. J. Binding mechanisms in supramolecular complexes. *Angew. Chem. Int. Ed*. **2009**, 48, 3924-3977.

(6) Qu, R. J.; Liu, H. X.; Feng, M. B.; Yang, X.; Wang, Z. Y. Investigation on intramolecular hydrogen bond and some thermodynamic properties of polyhydroxylated anthraquinones. *J. Chem. Eeg. Data* **2012**, 57, 2442-2455.

(7) Wash, P. L.; Ma, S.; Obst, U.; Rebek, J. J. Nitrogen-halogen intermolecular forces in solution. *J. Am. Chem. Soc.* **1999**, 121, 7973-7974.

(8) Ault, B. S. Infrared spectra of argon matrix-isolated alkali halide salt/water complexes. *J. Am. Chem. Soc.* **1978**, 100, 2426-2433.

(9) Bauer, S.; Tschirschwitz, S.; Lönnecke, P.; Frank, R.; Kirchner, B.; Clarke, M. L.; Hey-Hawkins, E. Enantiomerically pure bis(phosphanyl)carbaborane(12) compounds. *Eur. J. Inorg. Chem*. **2009**, 19, 2776-2788.

(10) Scheiner, S. A new noncovalent force: comparison of P ···N interaction with hydrogen and halogen bonds. *J. Chem. Phys*. **2011**, 134, 094315~1-094315~9.

(11) Scheiner, S. Can two trivalent N atoms engage in a direct N ···N noncovalent interaction? *Chem. Phys. Lett*. **2011**, 514, 32-35.

(12) Scheiner, S. On the properties of X ···N noncovalent interactions for first-, second-, and third-row X atoms. *J. Chem. Phys.* **2011**, 134, 164313~1-164313~9.

(13) Adhikari, U.; Scheiner, S. Comparison of PD (D = P, N) with other noncovalent bonds in molecular aggregates. *J. Chem. Phys*. **2011**,

135, 184306~1-184306~10.

(14) Scheiner, S.; Adhikari, U. Abilities of differentelectron donors (D) to engage in a P ··Ð noncovalent interaction. *J. Phys. Chem. A* **2011**, 115, 11101-11110.

(15) Scheiner, S. Weak H-bonds: comparisons of CH ··O to NH ··O in proteins and PH ··N to direct P ··N interactions. *Phys. Chem. Chem. Phys.* **2011**, 13, 13860-13872.

(16) Del Bene, J. E.; Alkorta, I.; Sánchez-Sanz, G.; Elguero, J. Structures, binding energies, and spin-spin coupling constants of geometric isomers of pnicogen homodimers $(PHFX)_2$, X = F, Cl, CN, CH_3, NC. *J. Phys. Chem. A* **2012**, 116, 3056-3060.

(17) Del Bene, J. E.; Alkorta, I.; Sánchez-Sanz, G.; Elguero, J. Homo- and heterochiral dimers $(PHFX)_2$, X = Cl, CN, CH_3, NC: to what extent do they differ? *Chem. Phys. Lett*. **2012**, 538, 14-18.

(18) Alkorta, I.; Sánchez-Sanz, G.; Elguero, J.; Del Bene, J. E. Exploring $(NH_2F)_2$, H_2FP:NFH_2, and $(PH_2F)_2$ potential surfaces: hydrogen bonds or pnicogen bonds? *J. Phys. Chem. A* **2013**, 117, 183-191.

(19) Scheiner, S. Sensitivity of noncovalent bonds to intermolecular separation: hydrogen, halogen, chalcogen, and pnicogen bonds. *Cryst. Eng. Comm.* **2013**, 15, 3119-3124.

(20) Bauzá, A.; Quiñonero, D.; Deya` P. M.; Frontera, A. Halogen bonding versus chalcogen and pnicogen bonding: a combined Cambridge structural database and theoretical study. *Cryst. Eng. Comm.* **2013**, 15, 3137-3144.

(21) Zukerman-Schpector, J.; Otero-de-la-Roza, A.; Luaña, V.; Tiekink, E. R. T. Supramolecular architectures based on As(lone pair) ··π(aryl) interactions. *Chem. Commun*. **2011**, 47, 7608-7610.

(22) Bauzá, A.; Quiñonero, D.; Deyà, P. M.; Frontera, A. Pnicogen-π complexes: theoretical study and biological implications. *Phys. Chem. Chem. Phys.* **2012**, 14, 14061-14066.

(23) Scheiner, S. Effects of substituents upon the P ··N noncovalent interaction: the limits of its strength. *J. Phys. Chem. A* **2011**, 115, 11202-11209.

(24) Liu, X.; Cheng, J.; Li, Q.; Li, W. Competition of hydrogen, halogen, and pnicogen bonds in the complexes of HArF with XH_2P (X = F, Cl, and Br). *Spectrochimica Acta Part A* **2013**, 101, 172-177.

(25) Adhikari, U.; Scheiner, S. Sensitivity of pnicogen, chalcogen, halogen and H-bonds to angular distortions. *Chem. Phys. Lett*. **2012**, 532, 31-35.

(26) Frisch, M. J.; Trucks G. W.; Schlegel, H. B.; Scuseria, G. E.; Robb, M. A.; Cheeseman, J. R.; Zakrzewski, V. G.; Montgomery, J. A.; Stratmann, R. E.; Burant, J. C.; Dapprich, S.; Millam, J. M.; Daniels, A. D.; Kudin, K. N.; Strain, M. C.; Farkas, O.; Tomasi, J.; Barone, V.; Cossi, M.; Cammi, R.; Mennucci, B.; Pomelli, C.; Adamo, C.; Clifford, S.; Ochterski, J.; Petersson, G. A.; Ayala, P. Y.; Cui, Q.; Morokuma, K.; Malick, D. K.; Rabuck, A. D.; Raghavachari, K.; Foresman, J. B.; Cioslowski, J.; Ortiz, J. V.; Stefanov, B. B.; Liu, G.; Liashenko, A.; Piskorz, P.; Komaromi, I.; Gomperts, R.; Martin, R. L.; Fox, D. J.; Keith, T.; Al-Laham, M. A.; Peng, C. Y.; Nanayakkara, A.; Gonzalez, C.; Hallacombe, M.; Gill, P. M. W.; Johnson, B. G.; Chen, W.; Wong, M. W.; Andres J. L.; Head-Gordon, M.; Replogle, E. S.; Pople, J. A. *Gaussian 03*, Gaussian, Inc., Wallingford CT **2003**.

(27) Scheiner, S. Effects of multiple substitution upon the P ··N noncovalent interaction. *Chem. Phys.* **2011**, 387, 79-84.

(28) Adhikari, U.; Scheiner, S. Effects of carbon chain substituents on the P ··N noncovalent bond. *Chem. Phys. Lett.* **2012**, 536, 30-33.

(29) Boys, S. F.; Bernardi, F. The calculation of small molecular interactions by the differences of separate total energies. Some procedures with reduced errors. *Mol. Phys.* **1970**, 19, 553-566.

(30) Lu, T.; Chen, F. W. Multiwfn: a multifunctional wavefunction analyzer. *J. Comput. Chem.* **2012**, 33, 580-592.

(31) Xu, H. Y.; Wang, W.; Zou, J. W. Theoretical study of pnicogen bonding interactions between PH_2X and five-membered heterocycles. *Acta Chim. Sinica* **2013**, 71, 1175-1182.

(32) Popelier, P. L. A. Characterization of a dihydrogen bond on the basis of the electron density. *J. Phys. Chem. A* **1998**, 102, 1873-1878.

(33) Grabowski, S. J. *Ab initio* calculations on conventional and unconventional hydrogen bonds study of the hydrogen bond strength. *J. Phys. Chem. A* **2001**, 105, 10739-10746.

(34) Scheiner, S.; Grabowski, S. J.; Kar, T. Influence of hybridization and substitution on the properties of the CH ··O hydrogen bond. *J. Phys. Chem. A* **2001**, 105, 10607-10612.

(35) Wang, W. Z. Halogen bond involving hypervalent halogen: CSD search and theoretical study. *J. Phys. Chem. A* **2011**, 115, 9294-9299.

(36) Lu, Y. X.; Zou, J. W.; Wang, Y. H.; Yu, Q. S. *Ab initio* and atoms in molecules analyses of halogen bonding with a continuum of strength. *J. Mol. Struct. (THEOCHEM)* **2006**, 776, 83-87.

(37) Lu, Y. X.; Zou, J. W.; Wang, Y. H.; Yu, Q. S. Theoretical investigations of the C-X/π interactions between benzene and some model halocarbons. *Chem. Phys*. **2007**, 334, 1-7.

(38) Johnson, E. R.; Keinan, S.; Mori-Sánchez, P.; Contreras-Garcá, J.; Cohen, A. J.; Yang, W. T. Revealing noncovalent interactions. *J. Am. Chem. Soc*. **2010**, 132, 6498-6506.

(39) Xu, H. Y.; Wang, W. Interaction between Mg-porphyrin and nitrogen, oxygen heterocyclic compounds. *Acta Phys. -Chim. Sin*. **2011**, 27, 2565-2570.

(40) Xu, H. Y.; Wang, W.; Xu, X. Y. Molecular recognition of pyromellitic imide-azacyclophane to organic pollutant. *Chin. J. Struct. Chem.* **2012**, 31, 591-598.

(41) Xu, L.; Lv, J.; Sang, P.; Zou, J. W.; Yu, Q. S.; Xu, M. B. Comparative insight into the halogen bonding of 4-chloropyridine and its metal [Cu^{I}, Zn^{II}] coordinations with halide ions: a theoretical study on M–C–X ···X'. *Chem. Phys.* **2011**, 379, 66-72.

(42) Grabowski, S. J. What is the covalency of hydrogen bonding? *Chem. Rev.* **2011**, 111, 2597-2625.

Investigation of the Substituent Effects on π-Type Pnicogen Bond Interaction

XU Hui-Ying(许惠英)　CAO Sheng-Wei(曹生炜)

WANG Wei(王　维)　ZHU Jian-Qing(朱建清)

ZOU Jian-Wei(邹建卫)　XU Xiao-Lu(许晓路)　LU Yin(陆　胤)

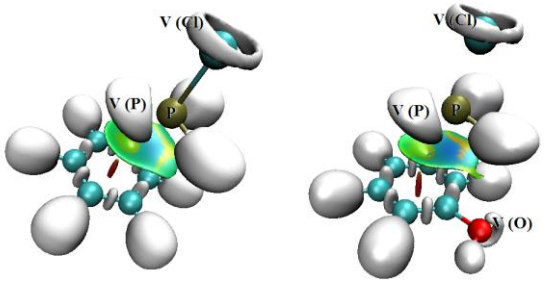

Complexes 1　　Complexes 2

RDG/ELF isosurface map can visualize the positions and strengths of the pnicogen bonding, as well as the spatial change of the electron localization upon the formation of complexes.